Development 128, 1109-1118 (2001)
Printed in Great Britain © The Company of Biologists Limited 2001
DEV2662

Establishment and maintenance of parasegmental compartments

Sarah C. Hughes and Henry M. Krause*

Banting and Best Department of Medical Research, Department of Molecular and Medical Genetics, University of Toronto, Charles H. Best Institute, 112 College Street, Toronto, Ontario, M5G 1L6, Canada
*Author for correspondence (e-mail: h.krause@utoronto.ca)

Accepted 15 January; published on WWW 13 March 2001

SUMMARY

Embryos of higher metazoans are divided into repeating units early in development. In *Drosophila*, the earliest segmental units to form are the parasegments. Parasegments are initially defined by alternating stripes of expression of the *fushi-tarazu* and *even-skipped* genes. How *fushi-tarazu* and *even-skipped* define the parasegment boundaries, and how parasegments are lost when *fushi-tarazu* or *even-skipped* fail to function correctly, have never been fully or properly explained. Here we show that parasegment widths are defined early by the relative levels of *fushi-tarazu* and *even-skipped* at stripe junctions. Changing these levels results in alternating wide and narrow parasegments. When shifted by 30% or more, the enlarged parasegments remain enlarged and the reduced parasegments are lost. Loss of the reduced parasegments occurs in three steps; delamination of cells from the epithelial layer, apoptosis of the delaminated cells and finally apoptosis of inappropriate cells remaining at the surface. The establishment and maintenance of vertebrate metameres may be governed by similar processes and properties.

Key words: Parasegment, *fushi tarazu*, *even-skipped*, Compartment, Apoptosis, *Drosophila melanogaster*

INTRODUCTION

One of the primary patterning decisions required in higher organisms is the division of the major body axis into serially repeating units or segments. This body architecture is apparent in the external features of invertebrates, and in the central nervous system and associated structures of vertebrates. In *Drosophila*, the first metameric divisions to be formed are referred to as parasegments. The borders of the 14 parasegments formed in the early embryo are shifted anteriorly with respect to the segmental borders that form later (Martinez-Arias and Lawrence, 1985; Lawrence, 1988).

The positions of odd and even-numbered parasegments are first defined by the expression patterns of two pair-rule genes, *fushi-tarazu* (*ftz*) and *even-skipped* (*eve*) (Lawrence et al., 1987; Lawrence and Johnston, 1989). Prior to gastrulation, *ftz* and *eve* are expressed in alternating stripes that are about four to five cells wide; *ftz* stripes define even-numbered parasegments and *eve* stripes define odd-numbered parasegments. At this stage, the blastoderm cells are otherwise undifferentiated. However, the expression of *ftz* and *eve* target genes such as segment polarity and homeotic selector genes soon results in distinct physical borders and unique parasegmental identities (Ingham and Martinez-Arias, 1986; Lawrence et al., 1987; Carroll et al., 1988a; Ingham et al., 1988; Irish et al., 1989; Peifer and Bejsovec, 1992).

Although it is clear from previous studies that *ftz* and *eve* define parasegmental boundaries, exactly how and when they do so has been a subject of debate. The earliest models suggested that *ftz* and *eve* position the parasegmental borders after gastrulation, about an hour after the two genes are first expressed (Lawrence et al., 1987; Lawrence and Johnston, 1989). This assumption was based on three observations; first, the borders of *ftz* and *eve* stripes are diffuse and overlapping before this time (Frasch and Levine, 1987; Kellerman et al., 1990; Ingham and Martinez Arias, 1992). Second, induction of the downstream target gene *engrailed* (*en*) coincides temporally and spatially with the resolution and intensification of anterior *ftz* and *eve* stripe borders (Lawrence et al., 1987; Ingham et al., 1988; Kellerman et al., 1990). Finally, in some of the first pair-rule phenotypes to be characterized, the anterior borders of *ftz* and *eve* stripes failed to intensify and sharpen (Howard and Ingham, 1986; Frasch and Levine, 1987; Carroll et al., 1988b; Carroll and Vavra, 1989). Subsequent studies, however, have shown that parasegmental borders can still form when the levels (or activities) of *ftz* and *eve* are altered and when their anterior stripe borders fail to sharpen (DiNardo and O'Farrell, 1987; Frasch et al., 1988; Kellerman et al., 1990; Manoukian and Krause, 1992; Lawrence and Pick, 1998; Nasiadka and Krause, 1999). An important consequence of these altered expression levels is that parasegment borders are shifted. One of the aims of this study was to determine how and when these shifts occur.

A second topic of some debate, and one that has not been properly explained is how *ftz* and *eve* pair-rule phenotypes are generated. For example, *ftz* mutants were first described as a fusion of alternate segments resulting in half the number of double-width segments (Wakimoto et al., 1984). A subsequent study (Struhl, 1985) described *ftz* mutants as having lost segment-wide regions that correspond closely to even-

numbered parasegments. Also characterized in this study was a pair-rule phenotype caused by ectopic expression of *ftz* (an 'anti-*ftz*' phenotype). This phenotype is described as a near-reciprocal deletion of odd-numbered parasegments. As with the *ftz* phenotype, the remaining parasegments were depicted as normal in width. The larvae arising from these embryos were depicted as half the length of wild-type larvae. Follow-up studies by Ish-Horowicz and colleagues (Ish-Horowicz and Gyurkovics, 1988) provided an alternative description of these phenotypes. It was postulated that *ftz*- and anti-*ftz* phenotypes are generated from the same double-wide segmental fusions as first described by Wakimoto and colleagues (Wakimoto et al., 1984), but that these composite regions are given alternate parasegment identities by the differential expression of homeotic selector genes. Another account of *ftz* and *eve* pair-rule mutants describes the remaining regions as non-composite, expanded parasegmental units (Martinez Arias and White, 1988).

These accounts are inconsistent in their interpretation of what regions are retained, and they do not explain how missing regions are physically removed. Magrassi and Lawrence (Magrassi and Lawrence, 1988) studied the latter problem by monitoring patterns of cell death in *ftz* mutant embryos. They observed increased numbers of dying cells dispersed within the ectoderm of both *ftz* and *eve* parasegments. Although the numbers of dying cells in the *ftz* parasegments were higher than normal, their numbers and positions did not clearly explain how these regions were removed. These issues are addressed here.

Our study focuses on how parasegmental boundaries are positioned and what happens when these boundaries are shifted. The results show that parasegmental widths are first defined well before the completion of cellularization by the relative levels of *ftz* and *eve* expression. Changing these relative levels in pre-cellularized embryos results in major changes in parasegment widths. However, *ftz* and *eve* expression levels can be changed quite dramatically with no effects on parasegmental boundaries so long as the relative levels are kept in balance. We also show that, when induced changes in parasegment width approach 30% or greater, they cannot correct back to normal. Enlarged parasegments remain enlarged and reduced parasegments are cleanly deleted. Removal of the reduced parasegments occurs by a previously undescribed three-step process. These observations explain the average 1.4- to 1.5-fold increase in size of the remaining parasegments and the 30-40% decrease in size of the mutant larvae.

MATERIALS AND METHODS

Drosophila stocks

The following stocks were used: the hypomorphic *eve* line $cn^1 eve^{ID19} bw^1 sp^1$/CyO, (referred to as eve^{ID19}; Frasch et al., 1988), the hypomorphic *ftz* line ftz^{54B}/TM3, the heat inducible *ftz* lines *hsf2* (Struhl, 1985) or *hsf245A* (Fitzpatrick et al., 1992), and the heat-inducible *eve* line, $hseve^{19B}$ (Manoukian and Krause, 1992). Oregon R flies were used as wild-type controls. Where required, a CyO balancer marked with a *hunchback lacZ* reporter (Driever et al., 1989) was used to identify non-homozygous progeny. Flies carrying 3rd chromosome *ftz-lacZ* reporters over TM3 (Hiromi et al., 1985) or 2nd chromosome *eve-lacZ* reporters over SM6 (Pazdera et al., 1998) were used in combination with eve^{ID19}, *hsf2* and $hseve^{19B}$ lines to follow the fates of *ftz*- and *eve*-expressing cells. eve^{ID19} and ftz^{54B} were obtained from the Bloomington Stock Centre. *hsf2* and $hseve^{19B}$ were obtained from Gary Struhl.

In situ hybridization

DNA probes for *en* and *reaper* were prepared by PCR as described by Nasiadka and Krause (Nasiadka and Krause, 1999). Hybridization and posthybridization washes were carried out as described by Saulier-Le Drean et al. (Saulier-Le Drean et al., 1998). When double-labeling for β-galactosidase and EN proteins, immunohistohemistry was carried out as described by Saulier-Le Drean et al. (Saulier-Le Drean et al., 1998).

Heat treatments

Embryos were collected for 30 minutes and aged at 25°C to appropriate stages. For individual treatments, *ftz* and *eve* temperature-sensitive alleles continued to be maintained at 25°C (partial inactivation), and heat inducible lines were given a 4 minute heat shock at the times stated by immersion in water at 36.5°C. Embryos for survival testing were raised at 25°C until 2.5-3 hours AEL (after egg laying) and then heat shocked for 4 minutes. Approximately 300-400 embryos were collected for each genetic background and then transferred to food vials and allowed to develop at 25°C. The percentage of larvae that hatched and the percentage of adults that eclosed were counted.

Measurement of parasegmental widths

To clearly mark each cell, embryos of the appropriate age were hybridized with an *en* DNA probe and immunohistohemistry (NBT/BCIP; see above) and then counterstained with the DNA specific dye bis-benzamide (1:10,000 dilution of a 5.0 mg/ml stock solution). The NBT/BCIP stain quenches the fluorescent bis-benzamide signal, clearly marking the *en* cells and parasegment borders. Measurements of cell numbers and the distances in microns (μm) from one *en* stripe to the next were obtained using a Zeiss Axioplan 2E microscope and Northern Eclipse™ image capture and analysis software (Empix Imaging, Mississauga, ON, Canada). Measurements were obtained for parasegments 3, 4, 5 and 6 along the ventral-lateral surface, four rows of cells above the ventral midline.

Detection of cell death

This procedure was adapted from that of Abrams et al. (Abrams et al., 1993). Embryos were suspended in equal volumes of heptane and a freshly prepared 10 μg/ml solution of Acridine Orange (prepared in 1× PBS) for 5 minutes. Embryos were then transferred to a new scintillation vial and fixed as described above for antibody staining. Immunofluorescent staining was carried out as described below.

Immunofluorescence and confocal microscopy

Embryos for immunofluorescence were collected and fixed as described above. Embryos were rinsed twice in methanol, then twice in PBTBB (1× PBS + 0.1% Tween 20 + 0.5% skim milk powder + 0.05% BSA). Blocking in PBTBB was carried out at room temperature for at least 2 hours. Primary antibodies (mouse α-EN 4D9 (1:1000), mouse α-WG 4D4 (1:10; Developmental Hybridoma Bank), rabbit α-spectrin (1:1,000; obtained from D. Branton) were diluted in PBTBB and incubated with embryos overnight at 4°C. After washing, appropriate combinations of the following secondary antibodies were incubated with embryos for 2 hours; α-mouse CY3 (1:1000), α-mouse CY2 (1:1,000), α-rabbit CY3 (1:1,500) and/or α-sheep CY3 (1:1,000; Jackson ImmunoResearch Laboratories Inc.). If two primary antibodies from the same species were used, one antibody was added first and then blocked with unconjugated sheep-α-mouse or sheep-α-rabbit antibodies (1:200; Jackson ImmunoResearch Laboratories Inc.) as per the manufacture's instructions. After incubation with secondary antibodies, embryos were washed in PBTBB, resuspended in 2.5%

DABCO (1,4-diazabicyclo [2.2.2.] octane) in 10% glycerol, mounted on slides and imaged using a Leica TCSNT confocal microscope.

RESULTS

Altering the relative levels of ftz and eve yields reciprocal pair-rule phenotypes

Previous studies have shown that *ftz* and *eve* pair-rule phenotypes can be generated by either raising or lowering the levels of *ftz* or *eve* expression (DiNardo and O'Farrell, 1987; Frasch and Levine, 1987; Laughon et al., 1988; Kellerman et al., 1990; Manoukian and Krause, 1992; Nasiadka and Krause, 1999). This is achieved using either temperature-sensitive lines (TS; eve^{ID19} or ftz^{54b}) or *hsp70* promoter-inducible transgenic lines (HS; $hseve^{19B}$, *hsf2* or *hsf245A*). For the two TS lines, the heat treatments used result in a partial loss of activity. For the heat inducible lines, levels of expression are boosted within normal stripes, and low levels of expression (25-50% of endogenous levels) are induced between stripes (Struhl, 1985; Manoukian and Krause, 1992; Copeland et al., 1996; data not shown). The latter inter-stripe expression is transient and, except at stripe borders (which are broadened), has no apparent consequences.

A benefit of these fly lines is that the timing and degree of gene activation/inactivation can be precisely controlled. In this way, we found that relatively early heat treatments (2.25-2.75 h AEL for the HS lines) could generate pair-rule phenotypes despite the early and persistent expression of all 14 stripes of the segment polarity gene *engrailed* (*en*; Fig. 1). Longer or later heat treatments generally cause the loss of half or all *en* stripes (Frasch and Levine, 1987; Frasch et al., 1988; Ish-Horowicz and Gyurkovics, 1988; Ish-Horowicz et al., 1989; Manoukian and Krause, 1992; data not shown). Nevertheless, the pair-rule phenotypes shown in Fig. 1, and those generated when half the *en* stripes are missing, are indistinguishable. The persistence of all 14 *en* stripes is a potentially important tool, as it permits the accurate monitoring of *ftz* and *eve* parasegment borders during later stages of embryonic development.

Three additional important points are apparent in Fig. 1. The first is that similar pair-rule phenotypes can be generated by either lowering the expression/activity levels (simplified to 'levels' hereafter) of *eve* (Fig. 1B) or raising the levels of *ftz* (Fig. 1C). Conversely, reciprocal pair-rule phenotypes are generated by either lowering the levels of *ftz* (Fig. 1D), or raising the levels of *eve* (Fig. 1E). The second point is that, while all 14 stripes of *en* are initially present in each of these heat-treated lines, these stripes are not evenly spaced. When the levels of *eve* are lowered (Fig. 1G) or *ftz* increased (Fig. 1H), there is an apparent increase in the width of *ftz*-dependent parasegments at the expense of *eve*-dependent parasegments (compare for example the distance between stripes 6 and 7 and stripes 7 and 8). The opposite phasing is observed when the levels of *eve* are increased (Fig. 1I) or the levels of *ftz* reduced (Fig. 1J). In the latter two cases, there is an increase in the width of *eve*-dependent parasegments at the expense of *ftz*-dependent parasegments. Taken together, these first two observations suggest that parasegment widths are determined by the relative levels of *ftz* and *eve*.

The third important feature is the length of the pair-rule cuticles produced. *ftz* and *eve* pair-rule phenotypes have been previously described as either fusions or deletions of alternate segmental regions. This implies the production of a cuticle that is either normal in length or half the normal length. The pair-rule cuticles in Fig. 1 are neither. They are, on average, about 70% the length of a wild-type cuticle, and the remaining segments are about 1.4 times wider than wild-type segments. This is also the case for *ftz* null cuticles, other *eve* hypomorphs

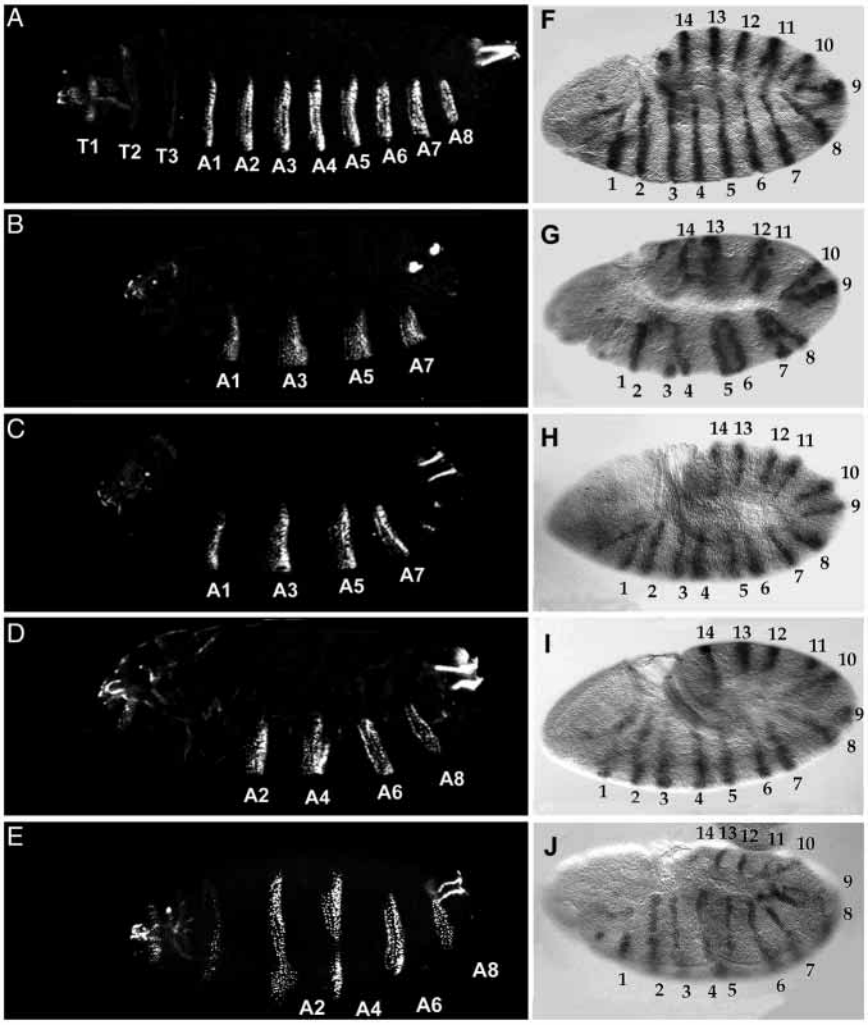

Fig. 1. Effects of *ftz* and *eve* on segmentation and parasegment width. (A-E) The pair-rule cuticular phenotypes that are generated when levels of *eve* or *ftz* are genetically altered. (F-J) Corresponding *en* expression patterns observed earlier in stage 9 embryos. A and F are wild type, B and G are an *eve* temperature-sensitive allele (eve^{ID19}), C and H are heat shock *ftz* (*hsf2*), D and I are heat shock *eve* ($hseve^{19B}$) and E and J are a *ftz* temperature sensitive allele (ftz^{54b}).

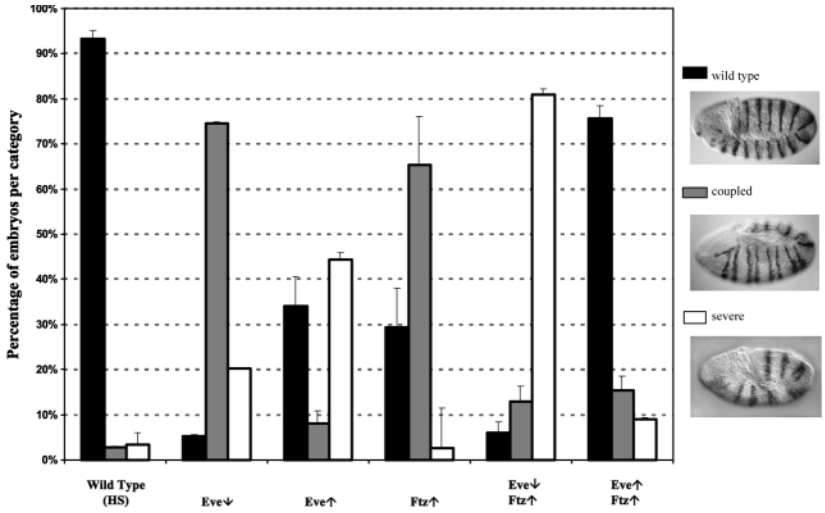

Fig. 2. Relative levels of *eve* and *ftz* are important. Levels of *eve* and *ftz* were genetically altered alone and in combination and the effects on EN expression patterns monitored. Values on the graph denote the percentages at which normal (black bars), coupled (gray bars) and more severe (fused or partially fused; white bars) En stripe expression patterns were observed (typical examples shown at right). Values are given for heat treated wild-type control, eve^{ID19}, (eve↓), $hseve^{19B}$ (eve↑), *hsf2* (ftz ↑), eve^{ID19}; *hsf245A* (eve↓ ftz ↑), and *hsf2*; $hseve^{19B}$ (eve↑ ftz↑) embryos. Error bars show standard deviation.

and phenotypes generated using later heat shocks (data not shown). The widths of the enlarged parasegments in the stage 9 embryos shown in Fig. 1G-J are also about 1.4 times wider than normal. If these parasegments were subsequently maintained, and the smaller parasegments lost, the resulting cuticles would be about 70% the length of a wild-type cuticle, as observed.

Parasegments are first defined by the expression domains of *ftz* and *eve* and soon after by stripes of expression of the segment polarity genes *en* and *wingless* (*wg*) and homeotic selector genes such as *Ultrabithorax* (*Ubx*) (Lawrence et al., 1987; Lawrence, 1988; Lawrence and Johnston, 1989). To test whether the shifted *en* stripes shown in Fig. 1 continue to mark parasegment borders, we also monitored the expression patterns of *ftz-lacZ* and *eve-lacZ* reporter genes, as well as patterns of *wg* and *Ubx* expression. Double-labeling with *en* showed that all four expression patterns shift along with *en* stripes when the levels of *ftz* and *eve* are altered (data not shown). Hence, the shifted *en* stripes continue to mark parasegmental boundaries. The relative positioning of *ftz-lacZ*, *eve-lacZ* and *Ubx* stripes is also the same in embryos that partially or completely lack alternate stripes of *en* (caused by longer or later heat treatments), indicating similar shifts in parasegment borders even when not marked by *en* (Ish-Horowicz et al, 1989; Manoukian and Krause, 1992, and data not shown).

Relative expression levels of *ftz* and *eve* position the parasegmental boundaries

The results shown in Fig. 1 suggest that the relative levels of *ftz* and *eve* determine the widths of alternate parasegments. To test this further, we altered the levels of *ftz* and *eve* in various combinations by combining genetic backgrounds and subjecting the 2.5- to 3-hour old progeny to a 4 minute heat pulse. The embryos were fixed 1 hour later (stage 9) and scored for normal and abnormal *en* expression patterns. Fig. 2 shows the percentage of embryos with normal (black bars), coupled (gray bars) or more severe (white bars; e.g. partial fusion of stripes) patterns of *en* expression (examples of each pattern are shown in the inset at right).

When *eve* levels are lowered or when *ftz* levels are raised, the majority of embryos exhibit a coupled pattern of *en* stripes (Fig. 2) as previously shown (Fig. 1). However, when *eve* is lowered and *ftz* raised, both at the same time, there is a major shift from coupled patterns to more severe patterns (Fig. 2). Conversely, when *ftz* and *eve* are both increased at the same time, the majority of embryos revert back from coupled and severe *en* patterns to normal stripe spacing (Fig. 2). A similar trend is observed when *ftz* and *eve* are both lowered at the same time (data not shown). Thus, absolute levels of *ftz* and *eve*, within the ranges tested, appear to be unimportant so long as the relative levels are kept in balance.

The *ftz* and *eve* genes are required for functions other than the proper positioning of *en* stripes. Hence, we were interested to see how the varied levels of *ftz* and *eve* generated in the previous experiment would affect overall viability. As expected, raising or lowering the levels of either gene in isolation dramatically lowered the number of embryos hatching and the numbers of adults eclosing (Fig. 3). These numbers were reduced further when the levels of *eve* were reduced at the same time that levels of *ftz* were increased (Fig. 3). Unexpectedly, when the levels of *ftz* and *eve* were both increased at the same time, viability returned to near wild-type control levels, both for the number of embryos hatching and the number of adults eclosing (Fig. 3). Again, similar results were obtained when *ftz* and *eve* were both lowered at the same time (although viability was not as high due to non-equivalency of the TS lines; data not shown). These results illustrate quite dramatically that it is the relative levels of *ftz* and *eve*, and not their absolute levels (within the limits tested), that define the width, identity, and function of alternate parasegments.

Consequences of altering parasegmental widths

As demonstrated above, pair-rule phenotypes can be generated when all 14 parasegments are initially present. To determine how alternate parasegments are lost, we monitored stripes of *en* during later stages of embryogenesis. Fig. 4A-E shows that wild-type embryos maintain equivalent widths between adjacent *en* stripes during all of the stages tested. Fig. 4F-J shows *en* stripes at equivalent stages in eve^{ID19} embryos. As shown in Fig. 1, *ftz*-dependent parasegments are initially enlarged and *eve*-dependent parasegments are reduced (Fig. 4F). The relative widths of enlarged and reduced parasegments remain relatively constant until germ-band retraction. Between

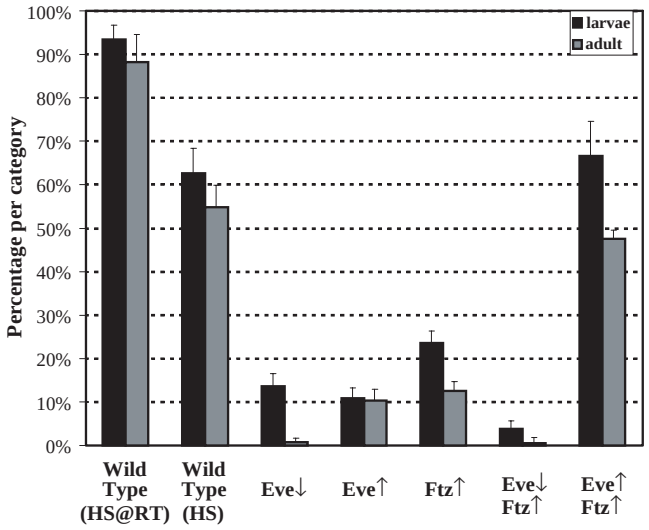

Fig. 3. Coordinate alterations in *ftz* and *eve* expression levels have little effect on viability. Expression levels of *ftz* and *eve* were altered as described in Fig. 2, and the embryos allowed to develop. Black bars indicate the percentage of embryos that hatch as 1st instar larvae. Gray bars indicate the percentage that eclose as adult flies. Combinations of *ftz* and *eve* under- and over-expressing lines are designated as in Fig. 2). Error bars show standard deviation.

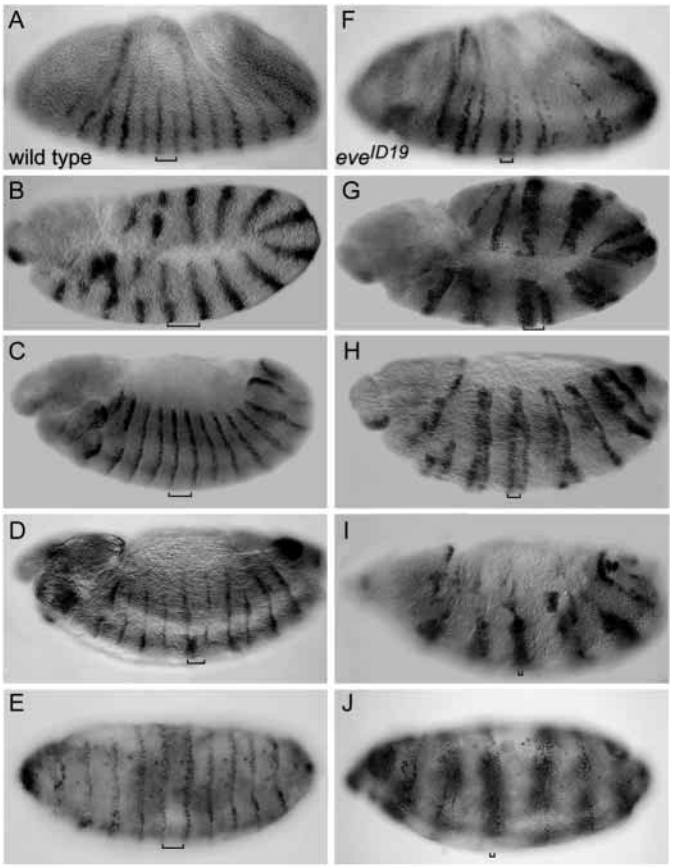

Fig. 4. Reduced parasegments are lost during germ band retraction. Expression patterns for EN are shown at successive stages of embryogenesis. (A-E) Wild-type embryos, (F-J) *eve*^{ID19} embryos. (A,F) Embryos at 3-3.5 h AEL (stage 8), (B,G) 7-7.5 h AEL (stage 11), (C,H) 9-9.5 h AEL (stage 12), (D,I) 12-12.5 h AEL (stage 15) and (E,J) 14-14.5 h AEL (stage 16). Braces denote the position of parasegment 5, an *eve*-dependent parasegment.

9 and 12 h AEL (stages 12-15) the relative widths of the smaller parasegments begin to decrease (Fig. 4H). By 12 h AEL (stage 15, Fig. 4I), gaps are seldom seen between the *en* stripes that mark the borders of odd-numbered parasegments. By 14 h AEL (stage 16; Fig. 4J) reduced parasegments are no longer observed and ectodermal *en* stripes are essentially wild-type in width (Fig. 4E; stripes appearing wider than normal are due to *en*-expressing cells below the ectodermal surface). At this point, the embryo is composed of seven enlarged parasegments, correlating well with the cuticle phenotype shown in Fig. 1B. Similar results were obtained with stripes of *wingless*, which are expressed just anteriorly to each *en* stripe (data not shown).

In order to monitor the process of parasegment loss more precisely, we measured the width of each parasegment and the number of cells across their widths from 3 h to 14 h AEL (stages 6-16). Fig. 5 shows these measurements in the form of stack graphs for parasegments 3, 4, 5 and 6 in wild-type, *eve*^{ID19}, *hsf2* and *hseve*^{19B} embryos. Average parasegment widths are shown on the left and cell counts on the right.

In wild-type embryos, each of the four parasegments contributes equally to the total number of cells and the total width of the four parasegments (Fig. 5A,B). In each of the mutant backgrounds, however, parasegments are already unequally spaced at 3-3.5 h AEL (when *en* stripes initiate; stage 6-7). The wide parasegments are on average about twice as wide as the narrow parasegments (about 1.4 times wider than wild-type versus 0.6 times wild-type, respectively). The wide parasegments also contain about twice the number of cells of the narrow parasegments (6 versus 3). The total width and number of cells in all four parasegments, however, is equivalent to wild type, indicating that early changes in cell fates are responsible for these shifts in width.

In each of the mutant backgrounds, the narrow parasegments maintain a constant relative width until around 9 h AEL (stage 12). After this time, they decrease further in both width and cell number. By 14 h AEL (stage 16), the narrow parasegments cease to exist. The wide parasegments, on the other hand, remain about 1.3-1.5 times wider and contain about 1.4 times as many cells as a normal parasegment. Taken together, these measurements illustrate that loss of the narrow parasegments is not due to changes in cell shape, size, or identity. Alternative possibilities are that cells within these parasegments die, fail to divide, move out of the ectodermal layer, or a combination of the three. Cells in the wide parasegments, on the other hand, appear to differentiate and divide as normal.

The role of cell death in parasegment loss

Previous studies of segmentation mutants have suggested that regions that normally express the mutant gene are deleted as a result of cell death (Ingham et al., 1985; Martinez-Arias and Ingham, 1985; Perrimon and Mahowald, 1987; Magrassi and Lawrence, 1988; Pazdera et al., 1998). To determine if cell death is responsible for loss of the reduced parasegments described here, Acridine Orange staining was used together with EN immunochemistry. Fig. 6A-E shows wild-type patterns of cell death at the relevant stages of embryogenesis. Apoptosis in the embryo normally begins at 7 h AEL (stage

11) and occurs in a fairly reproducible pattern that has been documented previously (Fig. 6A and Abrams et al., 1993; Pazdera et al., 1998). In the segmented regions of the embryo, the majority of cell death occurs between 9 and 11 h AEL (stages 12-14; Fig. 6B-D).

When the relative levels of *ftz* and *eve* are altered, a very different pattern of cell death is superimposed upon the normal pattern (Fig. 6F-J). Increased levels of apoptosis do not appear to be induced at or prior to 7 h AEL (stage 11) despite the earlier changes in parasegment size (Fig. 6F). By 9 h AEL (end of stage 12), however, higher than normal levels of cell death are observed (Fig. 6B,G). Surprisingly, the dying cells at this stage are almost exclusively in the wide parasegments with few, if any, dying cells detected in the narrow parasegments (Fig. 6G,H). Thus, both sets of parasegments appear to be compensating for their abnormal widths by altering their rates of apoptosis. However, as clearly shown by the cell counts and cuticular phenotypes, these changes in apoptotic frequencies are not sufficient to correct for the changes in width introduced.

By 11 h AEL (stage 14), overall levels of apoptosis within the ectodermal layer have decreased (Fig. 6I). However, clusters of dying cells begin to appear below the surface of the narrow parasegments (Fig. 6I, arrow). These clusters increase in size and number at 12 h AEL (stage 15; Fig. 6J). At this time, dying cells also begin to co-localize with EN in the newly fused stripes. This continues until the fused EN stripes attain a normal width (by approximately 14-15 h AEL).

In order to more clearly determine whether cells are dying within or below the ectodermal layer, confocal sections perpendicular to the embryo surface were obtained. Fig. 7 shows wild-type and *eve*^{ID19} embryos stained for EN (red), Wingless (WG; green), cell death (Acridine Orange; yellow) and ectodermal cell membranes (α-spectrin; blue). As the borders of the narrow parasegments begin to fuse, cells staining for EN and WG begin to appear below the ectodermal surface (Fig. 7E,F). Cells derived from the middle regions of the narrow parasegments, which stain for α-spectrin (normally restricted to ectodermal cells) but not EN or WG, are also present below the ectodermal surface (brace in Fig. 7F), clearly showing that cells of the narrow parasegments are delaminating and moving interiorly. In contrast, delaminating cells are rarely observed below the ectodermal surface of wild-type or broadened parasegments.

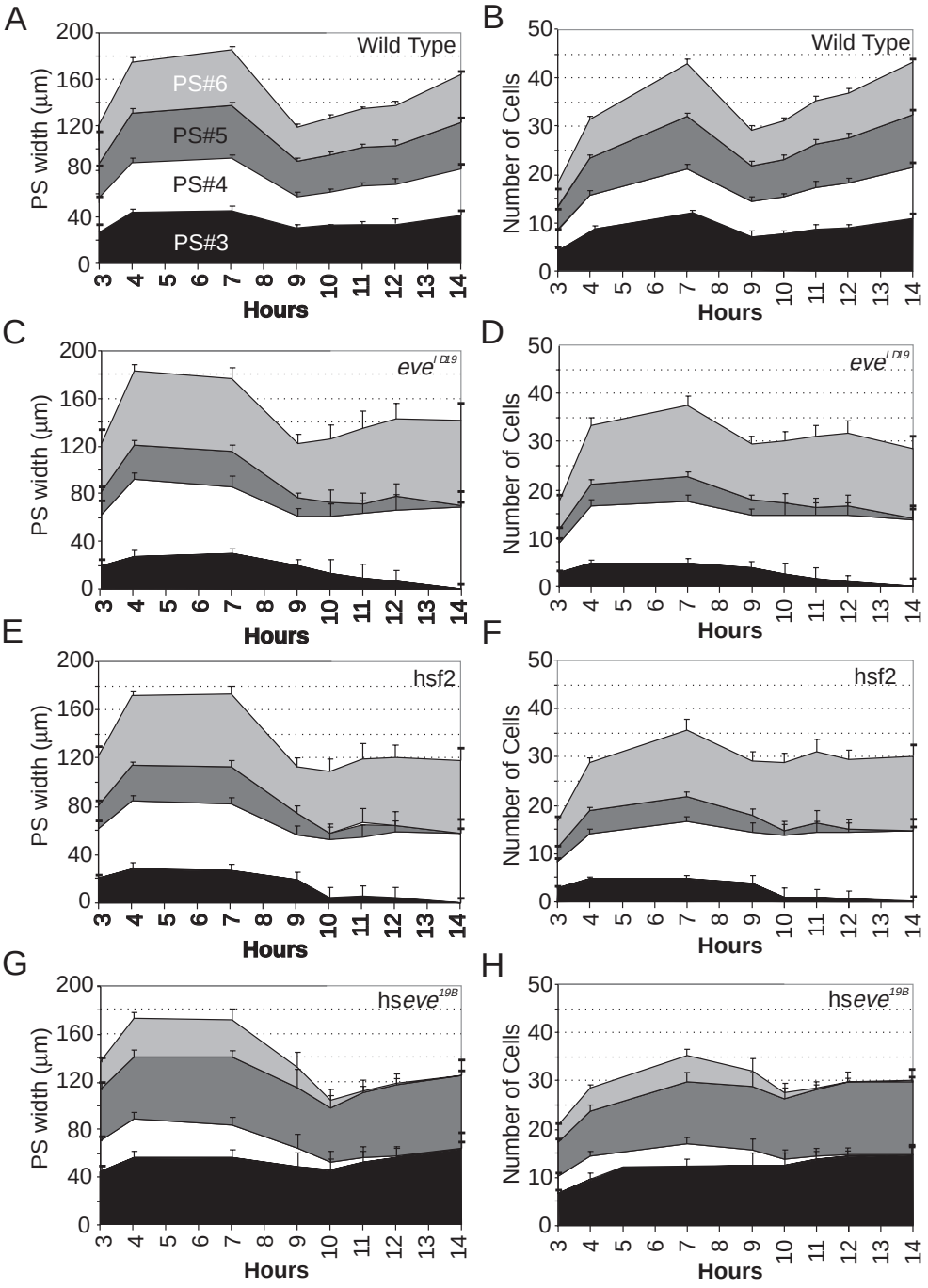

Fig. 5. Measurement of parasegmental widths and cell number in 3-14 h AEL (stages 6-16) embryos. (A,B) Wild type; (C,D) *eve*^{ID19}; (E,F) hsf2; (G,H) *hseve*^{19B}. Stacked area graphs (A,C,E,G) represent the average widths in microns (from one EN stripe to the next, see Materials and Methods) of four parasegments (PS; 3-6); (B,D,F,H) represent the average number of cells along the same paths in the same four parasegments. Each measurement represents a minimum of 50 embryos counted. Error bars show standard deviation.

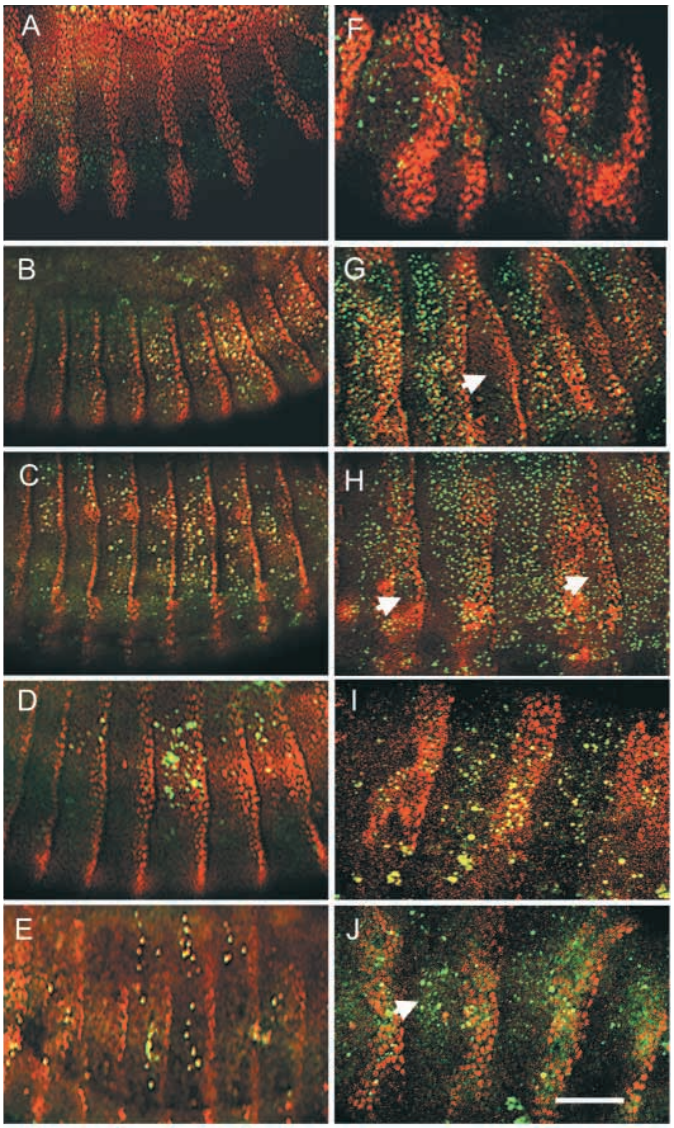

Fig. 6. Patterns of cell death in wild-type and mutant embryos. Embryos were double-labeled to show cell death, measured by Acridine Orange uptake (green), and parasegmental borders, outlined by expression of EN (red). (A-J) Close up lateral views of (A-E) wild-type embryos and (F-J) *eve*^{ID19} embryos. Embryos were analyzed at (A,F) 7-7.5 h AEL (stages 11;), (B,G) 9-9.5 h AEL (stage 12), (C,H) 10-10.5 h AEL (stage 13), (D,I) 11-11.5 h AEL (stage 14) and (E,J)12-12.5 h AEL (stage 15). The arrows in G and H indicate reduced parasegments. Arrow in J indicates clusters of apoptotic cells. The scale bar is equivalent to 15 μm and anterior is to the left.

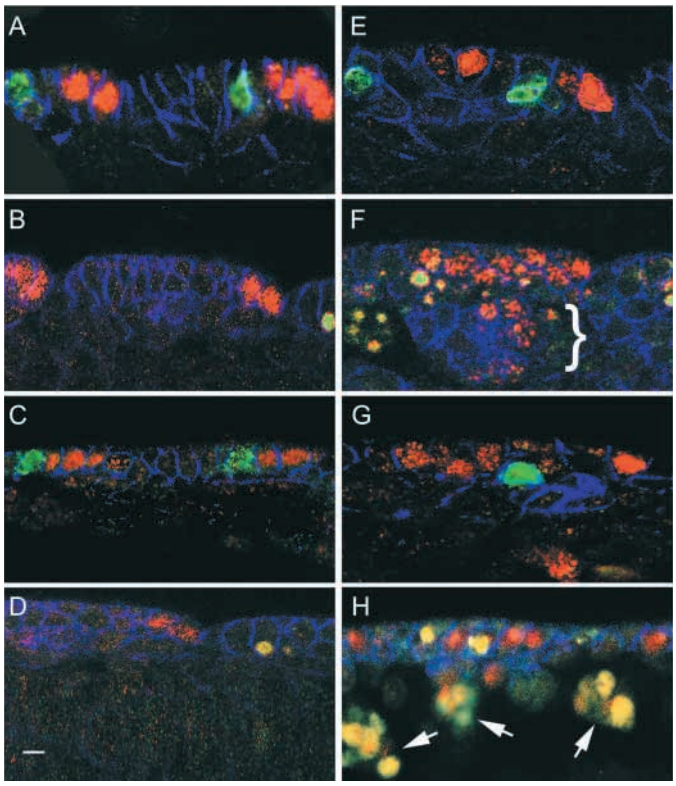

Fig. 7. Reduced parasegments are predominantly removed by delamination from the ectodermal surface. Embryos were triple-labeled and visualized by confocal microscopy to follow the fates of ectodermal cells. Optical sections through the ectodermal layer are shown with apical up and anterior to the left. In all panels, ectodermal cell membranes are stained blue (α-spectrin) and *en*-expressing cells are stained red. WG is shown in green in A,C,E and G. Acridine Orange-staining cells (yellow) are shown in B,D,F and H. (A-D) Wild-type embryos; (E-H) *eve*^{ID19} embryos. (A,B,E,F) 9-9.5 h AEL (stage 12) embryos; (C,D,G,H) 11-11.5 h AEL (stage 14) embryos. The bracket in F indicates spectrin-labelled cells that have delaminated from the ectoderm. The scale bar is equivalent to 5 μm.

In the same 9-9.5 h AEL mutant embryos, individual Acridine Orange-staining cells are seen within or just below the ectoderm of enlarged parasegments (Fig. 7F and data not shown). The cells that have delaminated from the surface of reduced parasegments, however, do not stain with Acridine Orange until 11-11.5 h AEL. At this time, large clusters of dying cells begin to appear below the ectodermal surface (Fig. 7H). With time, these clusters move away from the sites of delamination and break apart. At about the same time, *en*-expressing cells in the fused stripes also begin to stain with Acridine Orange (Fig. 7H). They then move out of the ectoderm, eventually yielding stripes of EN that are a normal 1-2 cells in width (see Fig. 4H). Occasionally, single cells or cell clusters are observed above the plane of the reduced parasegment ectodermal layer. This movement of cells outward may occur more frequently than observed, as these cells are likely to be lost after removal of the vitelline membrane.

In summary, the majority of cells in the reduced parasegments are not lost due to cell death. In fact, the frequency of apoptotic events in reduced parasegment ectoderm is dramatically reduced. Instead, the reduced segments are lost due to delamination from the ectodermal surface. Only after delaminating do the cells begin to die. An exception is the limited number of apoptotic events confined to the fused EN stripes that is required to reduce them to normal widths.

In situ hybridization with probes to *reaper* (data not shown) confirms that Acridine Orange stained cells do indeed represent cells that are dying via apoptosis and that, for the vast majority of cells in the reduced parasegments, this process does not initiate until after the cells have delaminated. HSFtz and *ftz* null

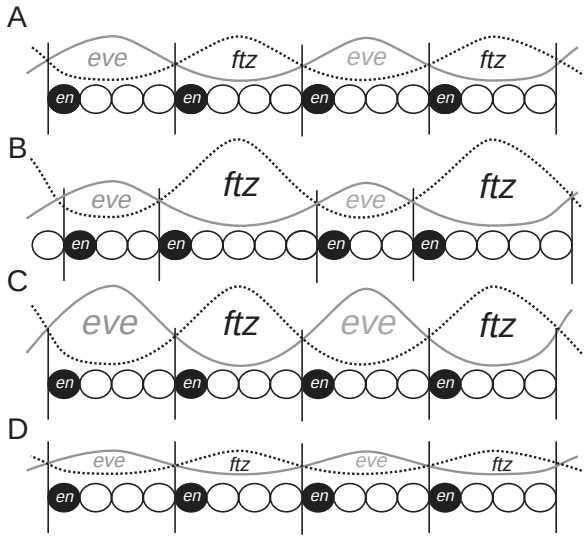

Fig. 8. A model for the positioning of parasegmental borders by *ftz* and *eve* expression. Early (late stage 5) expression patterns of *ftz* and *eve* are indicated as sinusoidal waves. Parasegment borders, indicated by vertical lines, form at the points where *ftz* and *eve* expression levels are equivalent. In wild-type embryos (A) this results in evenly spaced borders. B shows the result predicted when *eve* expression levels are decreased or *ftz* expression levels are increased. C shows the result expected when expression levels of both genes are simultaneously increased, and D shows the result expected when expression of both genes is simultaneously reduced.

embryos, in which alternate *en* stripes are missing, have the regions corresponding to reduced parasegments deleted in the same way (data not shown). Cells in these regions do not die until after delamination from the cell surface.

DISCUSSION

A new model for the definition of parasegment size

Previous studies have shown that *ftz* and *eve* are the primary determinants of parasegmental boundaries and identities (even versus odd; Lawrence et al., 1987; Lawrence and Johnston, 1989). Until quite recently, it was believed that the two genes perform these roles relatively late (stages 6-7), and that high levels and sharp anterior stripe boundaries are crucial (Lawrence and Johnston, 1989). Here, we show that, when in the right proportions, the absolute levels of *ftz* and *eve* are not particularly important. We also show that *ftz* and *eve* first define the positions of parasegment borders prior to the completion of cellularization (mid stage 5). At this time, *ftz* and *eve* stripes have a bell-shaped distribution across each stripe, and the stripes overlap with one another at their edges (Fig. 8; Frasch and Levine, 1987; Kellerman et al., 1990; Ingham and Martinez Arias, 1992). We suggest that parasegment boundaries occur at the points where stripes intersect and activity levels are equivalent (Fig. 8A). If the activity of one gene is raised while the other remains unchanged, these positions of equivalency move (Fig. 8B). The result is an alternating set of narrow and wide parasegments. These shifts become more pronounced with greater changes in activity or when both genes change in opposite directions. However, if both gene activities are increased (Fig. 8C) or decreased (Fig. 8D) at the same time the positions of equivalency do not change, and parasegments remain equal in width.

We suggest that the transition from overlapping stripe boundaries to sharp non-overlapping boundaries occurs via a combination of autoregulatory and mutually antagonistic functions. For example, if above a certain relative threshold level, FTZ autoregulation dominates over repression by EVE, and *ftz* expression rises to maximal levels while *eve* expression is lost. If below that relative threshold, repression by EVE dominates over FTZ autoregulation and *ftz* expression is lost while *eve* rises to maximal levels. The ability of FTZ and EVE to autoregulate and to mutually repress one another (directly or indirectly) has been well documented (Hiromi et al., 1985; Hiromi and Gehring, 1987; Frasch et al., 1988; Hoey and Levine, 1988; Goto et al., 1989; Kellerman et al., 1990; Manoukian and Krause, 1992; Klingler and Gergen, 1993; Fujioka et al., 1995; Nasiadka and Krause, 1999). Once the borders of *ftz* and *eve* stripes are established, combinatorial interactions with other segmentation gene products then determine where downstream targets such as *en* and *wg* are activated or repressed, thereby locking in the positions of the parasegment boundaries.

New explanations for *ftz* and *eve* pair-rule phenotypes

As detailed in the introduction, *ftz* and *eve* pair-rule phenotypes have been described and explained in a number of conflicting ways (Wakimoto et al., 1984; Struhl, 1985; Ish-Horowicz and Gyurkovics, 1988; Magrassi and Lawrence, 1988). We show here that the remaining cuticle is not simply composed of every second parasegment, nor is it composed of double-width or homeotically re-transformed segments. A relative decrease in *ftz* or *eve* activity causes a decrease in width of alternate parasegments and a corresponding expansion of adjacent parasegments. The smaller parasegments are excised and the enlarged parasegments retained. Efficient deletion (greater than 90%) of the reduced parasegments occurs when they are reduced by 30% or more. Enlarged parasegments are 1.4-1.5 times wider than normal parasegments. This degree of enlargement remains the same when levels of FTZ or EVE are increased further or when the levels of FTZ are reduced to zero (*eve* nulls affect all parasegments due to earlier roles). We suggest that these maximal widths reflect the edges of stage 5 *ftz* and *eve* stripes, beyond which autoregulation cannot occur. Further expansion of these stripes may be limited by the actions of other pair-rule or gap gene products. The resulting larva is composed of half the normal number of segments, but these are 1.3-1.5 times wider than normal segments, giving an overall length that is about 65-75% the length of a normal larva.

Parasegments have a limited ability to compensate for alterations in size

Parasegments are considered to be the first ‘compartments’ to form within the embryo (Lawrence and Morata, 1994). Compartments are fields of cells that originate from a common group of founder cells and that remain defined in lineage thereafter (Garcia-Bellido et al., 1973; Crick and Lawrence,

1975). Cells within adjoining compartments do not mix, most likely due to differential adhesion properties (Crick and Lawrence, 1975; Morata and Lawrence, 1977; Lumsden, 1990; Ingham and Martinez Arias, 1992; Dahmann and Basler, 1999). Compartments are further defined by unique gene expression patterns (e.g. *ftz* and *eve*) that respect their boundaries (Morata and Lawrence, 1977; Ingham and Martinez Arias, 1992; Lawrence and Morata, 1994).

Another property of compartments relevant to this study is that they are capable of sensing and modulating their size. Changes in size can be induced by injury, transplantation, irradiation, or genetic manipulation (Simpson and Morata, 1981; Wright and Lawrence, 1981; Frohnhofer and Nusslein-Volhard, 1986; Berleth et al., 1988; Driever and Nusslein-Volhard, 1988a; Driever and Nusslein-Volhard, 1988b; Yasuda et al., 1991; Busturia and Lawrence, 1994; Namba et al., 1997). In the case of reductions in size, compensation is most often in the form of increased cellular proliferation, and when increased in size, by programmed cell death.

Our studies show that parasegments can compensate for changes in size, but that this ability is relatively limited. Both reduced and enlarged parasegments showed changes in the normal numbers of apoptotic events. Dying cells were rarely seen in the ectoderm of reduced parasegments while higher than normal numbers were seen in enlarged parasegments. The numbers of dying cells and the time of onset were proportional to the degree of parasegment enlargement. These changes, however, were insufficient to compensate for the changes in widths induced in this study.

We also found that changes in mitotic frequency, as an alternate form of compensation, did not occur. Once established, the ratio of the number of cells per mutant parasegment, as compared to wild-type segments, remained relatively constant until cells in the reduced segments began to delaminate. This finding agrees with those obtained previously by increasing the number of copies of the *bicoid* gene (Busturia and Lawrence, 1994; Namba et al., 1997). Reduced parasegments in the compacted middle of the embryo failed to compensate by increasing rates of mitosis. However, these changes in width were usually subtle enough (<20%) that most segments were able to recover by reducing their rates of apoptosis (Namba et al., 1997). Our results show that once these changes reach 30% or higher, variations in apoptotic frequencies can no longer compensate.

Why do reduced parasegments delaminate?

One of the most novel and intriguing findings of this study was the unstable nature of reduced parasegments and the manner in which they were removed. Unlike previous explanations, we found that this occurred via a three-step process. First, large patches of cells moved out of the ectodermal layer. Next, they pinched off from the overlying ectoderm and then programmed cell death was initiated. Finally, the fused *engrailed* stripes remaining at the surface were resolved by late and sporadic apoptotic events. Although the precise spatial and temporal details of this process varied between individual embryos and different mutant backgrounds, the general trends and final consequences were the same.

The delamination of reduced parasegment cells occurred primarily during the late stages of germ band retraction. This coincidence between reduced parasegment delamination and germ band retraction suggests the possibility that cellular movement and adhesion may play a prominent role in the delamination process. During germ band retraction, normal parasegments are reduced in width by almost half (approx. 11 cells to 7). In reduced parasegments, the corresponding decrease results in an average width of just 3 cells. This reduced width means significantly fewer contacts with other reduced parasegment cells and more contacts with the cells of neighboring parasegments. This may drive the reduced parasegment cells to increase homogeneous contacts by forming spheres, much as observed in imaginal disks when small clones of anterior compartment identity are formed in the posterior compartment (Lawrence, 1997).

Molecules that provide differential adhesion have long been hypothesized to exist within and between different clonal compartments (Crick and Lawrence, 1975; Morata and Lawrence, 1977; Lumsden, 1990; Ingham and Martinez Arias, 1992). Their purpose would be to prevent cell mixing and to maintain straight compartment boundaries. Evidence for both adhesive and repulsive molecules in compartment boundary maintenance is currently strongest for vertebrate rhombomeres and somites (Guthrie and Lumsden, 1991; Klein, 1999; Mellitzer et al., 1999; Xu et al., 1999). The molecules responsible for these differential adhesion properties may have homologues that are expressed in *Drosophila* parasegments. Conversely, many of the compartmental properties described here may be shared by rhombomeres and somites.

We would like to thank Derek Van Der Kooy, Craig Smibert and Andrew Simmonds for comments on the manuscript. We would also like to thank Andrew Simmonds for assistance with figure preparations and Andrzej Nasiadka for fly stocks. Primary antibodies were obtained from the Developmental Studies Hybridoma Bank (NCIHD). Support for this work was provided by the National Cancer Institute of Canada.

REFERENCES

Abrams, J. M., White, K., Fessler, L. I. and Steller, H. (1993). Programmed cell death during *Drosophila* embryogenesis. *Development* **117**, 29-43.

Berleth, T., Burri, M., Thoma, G., Bopp, D., Richstein, S., Frigerio, G., Noll, M. and Nusslein-Volhard, C. (1988). The role of localization of bicoid RNA in organizing the anterior pattern of the Drosophila embryo. *EMBO J.* **7**, 1749-1756.

Busturia, A. and Lawrence, P. A. (1994). Regulation of cell number in Drosophila. *Nature* **370**, 561-563.

Carroll, S. B., DiNardo, S., PH, O. F., White, R. A. and Scott, M. P. (1988a). Temporal and spatial relationships between segmentation and homeotic gene expression in Drosophila embryos: distributions of the fushi tarazu, engrailed, Sex combs reduced, Antennapedia, and Ultrabithorax proteins. *Genes Dev.* **3**, 350-360.

Carroll, S. B., Laughon, A. and Thalley, B. S. (1988b). Expression, function, and regulation of the hairy segmentation protein in the Drosophila embryo. *Genes Dev.* **7**, 883-890.

Carroll, S. B. and Vavra, S. H. (1989). The zygotic control of *Drosophila* pair-rule gene expression. *Development* **3**, 673-683.

Copeland, J. W., Nasiadka, A., Dietrich, B. H. and Krause, H. M. (1996). Patterning of the *Drosophila* embryo using a homeodomain-deleted FTZ polypeptide. *Nature* **379**, 162-165.

Crick, F. H. and Lawrence, P. A. (1975). Compartments and polyclones in insect development. *Science* **189**, 340-347.

Dahmann, C. and Basler, K. (1999). Compartment boundaries: at the edge of development. *Trends Genet*. **15**, 320-326.

DiNardo, S. and O'Farrell, P. H. (1987). Establishment and refinement of segmental pattern in the Drosophila embryo: spatial control of engrailed expression by pair-rule genes. *Genes Dev.* **1**, 1212-1225.

Driever, W., Ma, J., Nusslein-Volhard, C. and Ptashne, M. (1989). Rescue of bicoid mutant Drosophila embryos by bicoid fusion proteins containing heterologous activating sequences. *Nature* **342**, 149-154.

Driever, W. and Nusslein-Volhard, C. (1988a). The bicoid protein determines position in the Drosophila embryo in a concentration-dependent manner. *Cell* **54**, 95-104.

Driever, W. and Nusslein-Volhard, C. (1988b). A gradient of bicoid protein in Drosophila embryos. *Cell* **54**, 83-93.

Fitzpatrick, V. D., Percival-Smith, A., Ingles, C. J. and Krause, H. M. (1992). Homeodomain-independent activity of the fushi tarazu polypeptide in Drosophila embryos. *Nature* **6370**, 610-612.

Frasch, M. and Levine, M. (1987). Complementary patterns of even-skipped and fushi tarazu expression involve their differential regulation by a common set of segmentation genes in Drosophila. *Genes Dev.t* **9**, 981-995.

Frasch, M., Warrior, R., Tugwood, J. and Levine, M. (1988). Molecular analysis of even-skipped mutants in Drosophila development. *Genes Dev.* **12B**, 1824-1838.

Frohnhofer, H. G. and Nusslein-Volhard, C. (1986). Organization of the anterior pattern in the *Drosophila* embryo by the maternal gene *bicoid*. *Nature* **324**, 120-125.

Fujioka, M., Jaynes, J. B. and Goto, T. (1995). Early even-skipped stripes act as morphogenetic gradients at the single cell level to establish engrailed expression. *Development* **12**, 4371-4382.

Garcia-Bellido, A., Ripoll, P. and Morata, G. (1973). Developmental compartmentalisation of the wing disk of Drosophila. *Nat. New Biol.* **245**, 251-253.

Goto, T., Macdonald, P. and Maniatis, T. (1989). Early and late periodic patterns of even skipped expression are controlled by distinct regulatory elements that respond to different spatial cues. *Cell* **3**, 413-422.

Guthrie and Lumsden, A. (1991). Formation and regeneration of rhombomere boundaries in the developing chick hindbrain. *Development* **112**, 221-229.

Hiromi, Y. and Gehring, W. J. (1987). Regulation and function of the Drosophila segmentation gene fushi tarazu. *Cell* **50**, 963-974.

Hiromi, Y., Kuroiwa, A. and Gehring, W. J. (1985). Control elements of the Drosophila segmentation gene fushi tarazu. *Cell* **43**, 603-613.

Hoey, T. and Levine, M. (1988). Divergent homeo box proteins recognize similar DNA sequences in Drosophila. *Nature* **6167**, 858-861.

Howard, K. and Ingham, P. (1986). Regulatory interactions between the segmentation genes fushi tarazu, hairy, and engrailed in the Drosophila blastoderm. *Cell* **6**, 949-957.

Ingham, P. W., Baker, N. E. and Martinez-Arias, A. (1988). Regulation of segment polarity genes in the Drosophila blastoderm by fushi tarazu and even skipped. *Nature* **331**, 73-75.

Ingham, P. W., Howard, K. R. and Ish-Horowicz, D. (1985). Transcription pattern of the *Drosophila* segmentation gene *hairy*. *Nature* **318**, 439-445.

Ingham, P. W. and Martinez Arias, A. (1992). Boundaries and fields in early embryos. *Cell* **68**, 221-235.

Ingham, P. W. and Martinez-Arias, A. (1986). The correct activation of Antennapedia and bithorax complex genes requires the fushi tarazu gene. *Nature* **6097**, 592-597.

Irish, V. F., Martinez-Arias, A. and Akam, M. (1989). Spatial regulation of the Antennapedia and Ultrabithorax homeotic genes during Drosophila early development. *EMBO J.* **8**, 1527-1537.

Ish-Horowicz, D. and Gyurkovics, H. (1988). Ectopic segmentation gene expression and metameric regulation in *Drosophila*. *Development* **Supplement 104**, 67-73.

Ish-Horowicz, D., Pinchin, S. M., Ingham, P. W. and Gyurkovics, H. G. (1989). Autocatalytic ftz activation and metameric instability induced by ectopic ftz expression. *Cell* **57**, 223-232.

Kellerman, K. A., Mattson, D. M. and Duncan, I. (1990). Mutations affecting the stability of the fushi tarazu protein of Drosophila. *Genes Dev.* **11**, 1936-50.

Klein, R. (1999). Bidirectional signals establish boundaries. *Curr. Biol.* **9**, R691-R694.

Klingler, M. and Gergen, J. P. (1993). Regulation of runt transcription by Drosophila segmentation genes. *Mech. Dev.* **43**, 3-19.

Laughon, A., Howell, W. and Scott, M. P. (1988). The interaction of proteins encoded by *Drosophila* homeotic and segmentation genes with specific DNA sequences. *Development* **104**, 75-83.

Lawrence, P. A. (1988). The present status of the parasegment. *Development Supplement* **104**, 61-65.

Lawrence, P. A. (1997). Developmental biology. Straight and wiggly affinities. *Nature* **389**, 546-547.

Lawrence, P. A. and Johnston, P. (1989). Pattern formation in the Drosophila embryo: allocation of cells to parasegments by even-skipped and fushi tarazu. *Development* **4**, 761-767.

Lawrence, P. A., Johnston, P., Macdonald, P. and Struhl, G. (1987). Borders of parasegments in Drosophila embryos are delimited by the fushi tarazu and even-skipped genes. *Nature* **328**, 440-442.

Lawrence, P. A. and Morata, G. (1994). Homeobox genes: their function in Drosophila segmentation and pattern formation. *Cell* **78**, 181-189.

Lawrence, P. A. and Pick, L. (1998). How does the fushi tarazu gene activate engrailed in the Drosophila embryo? *Dev. Genet.* **23**, 28-34.

Lumsden, A. (1990). The cellular basis of segmentation in the developing hindbrain. *Trends Neurosci*. **13**, 329-335.

Magrassi, L. and Lawrence, P. A. (1988). The pattern of cell death in fushi tarazu, a segmentation gene of *Drosophila*. *Development* **3**, 447-451.

Manoukian, A. S. and Krause, H. M. (1992). Concentration-dependent activities of the even-skipped protein in Drosophila embryos. *Genes & Development* **9**, 1740-1751.

Martinez Arias, A. and White, R. (1988). Ultrabithorax and engrailed expression in Drosophila embryos mutant for segmentation genes of the pair-rule class. *Development* **102**, 325-338.

Martinez-Arias, A. and Ingham, P. W. (1985). The origin of pattern duplications in segment polarity mutants of Drosophila melanogaster. *J. Embryol. Exp. Morphol.* **87**, 129-135.

Martinez-Arias, A. and Lawrence, P. A. (1985). Parasegments and compartments in the Drosophila embryo. *Nature* **313**, 639-642.

Mellitzer, G., Xu, Q. and Wilkinson, D. G. (1999). Eph receptors and ephrins restrict cell intermingling and communication. *Nature* **400**, 77-81.

Morata, G. and Lawrence, P. A. (1977). Homoeotic genes, compartments and cell determination in Drosophila. *Nature* **265**, 211-216.

Namba, R., Pazdera, T. M., Cerrone, R. L. and Minden, J. S. (1997). Drosophila embryonic pattern repair: how embryos respond to bicoid dosage alteration. *Development* **124**, 1393-1403.

Nasiadka, A. and Krause, H. M. (1999). Kinetic analysis of segmentation gene interactions in drosophila embryos. *Development* **126**, 1515-1526.

Pazdera, T. M., Janardhan, P. and Minden, J. S. (1998). Patterned epidermal cell death in wild-type and segment polarity mutant Drosophila embryos. *Development* **125**, 3427-3436.

Peifer, M. and Bejsovec, A. (1992). Knowing your neighbors: Cell interactions determine intrasegmental patterning in *Drosophila*. *Trends Genet.* **8**, 243-249.

Perrimon, N. and Mahowald, A. P. (1987). Multiple functions of segment polarity genes in Drosophila. *Dev. Biol.* **2**, 587-600.

Saulier-Le Drean, B., Nasiadka, A., Dong, J. and Krause, H. M. (1998). Dynamic changes in the functions of Odd-skipped during early *Drosophila* embryogenensis. *Development* **125**, 4851-4861.

Simpson, P. and Morata, G. (1981). Differential mitotic rates and patterns of growth in compartments in the Drosophila wing. *Dev. Biol.* **2**, 299-308.

Struhl, G. (1985). Near-reciprocal phenotypes caused by inactivation or indiscriminate expression of the Drosophila segmentation gene ftz. *Nature* **318**, 677-680.

Wakimoto, B. T., Turner, F. R. and Kaufman, T. C. (1984). Defects in embryogenesis in mutants associated with the antennapedia gene complex of Drosophila melanogaster. *Dev. Biol.* **102**, 147-172.

Wright, D. A. and Lawrence, P. A. (1981). Regeneration of the segment boundary in Oncopeltus. *Dev. Biol.* **85**, 317-327.

Xu, Q., Mellitzer, G., Robinson, V. and Wilkinson, D. G. (1999). In vivo cell sorting in complementary segmental domains mediated by Eph receptors and ephrins. *Nature* **399**, 267-271.

Yasuda, G. K., Baker, J. and Schubiger, G. (1991). Temporal regulation of gene expression in the blastoderm Drosophila embryo. *Genes Dev.* **5**, 1800-1812.